IJISET - International Journal of Innovative Science, Engineering & Technology, Vol. 3 Issue 5, May 2016.
www.ijiset.com

ISSN 2348 – 7968

Influence of Density Ratio on Turbulence in Two Phase Flow

Sherry K. Amedorme[1] & Joseph Apodi[2]

[1]School of Mechanical Engineering, Institute of Thermofluids and Combustion, University of Leeds, UK
Email: smedorme@yahoo.com

[2]Bolgatanga Polytechnic, P. O Box 767, Bolgatanga, Upper East Region, Ghana
Email: joeapodi@bpoly.edu.gh

Abstract

An entirely Eulerian approach treating two phase flow as a single phase with large scale features of the flow dependent only upon density variation is carried out. The average density for the two fluids is defined in the Computational Fluid Dynamics (CFD commercial code STAR-CCM+ and a transport equation tracking the liquid mass fraction models the turbulent mixing of liquid. Standard k-epsilon model is used for the turbulence. The paper shows the results of average density on turbulence and presents the contour plots of flow and turbulence fields such as turbulent kinetic energy and its rate of dissipation. The variations in the density ratios in relation to turbulent parameters are also presented and the noticeable changes in the turbulent quantities are analysed.

Key words: *Eulerian Model, Density Ratio, Liquid Mass Fraction, Turbulent and Flow Fields*

1. Introduction

Two-phase flows are encountered in a wide range of flow configurations, including separated flows, porous media flows, bubbly flows, slurry flows, and gas-particle and gas-droplet flows.There are two main approaches to handle the dispersed phase in the two-phase flow models, namely the Lagrangian and the Eulerian approaches. In the Lagrangian approach, the dispersed phase is treated by solving Lagrangian equations of motion for the particles with a prescribed set of initial conditions. Once the flow properties of the particles are known, the interface quantities between the two phases can be calculated. In the Eulerian approach, the dispersed phase is treated as an interacting and interpenetrating continuum. In this approach the governing equations for the two phases are quite similar to the well-known Navier-Stokes equations. These equations are coupled primarily by three mechanisms, the mass exchange, the displacement of the carrier phase by the volume occupied by particles, and momentum interchange between particles and the carrier phase. Many two-way coupling studies are presented in the literature, based either on the Lagrangian or Eulerian approaches [1-4]. Of most importance, the continuum assumption is justified when using the Eulerian approach. However, within the Eulerian methods, the two phase model approach is complex to model as high number of equations are solved as each fluid is transported. On the other hand, entirely one-fluid Eulerian model proposed by Vallet et al [5] has advantage to compute only the transport of one single fluid with high density variation. Many authors [6-8] have studied density variations in two phase flow in relation to turbulence but did not show explicitly the effect of density ratio on the individual turbulent parameters. However, they indicated that there are two main kinds of density variation: the first originates in the compressibility effects induced by high-velocity flows and the second results from the mixing of several different fluids (gas or liquid) with different densities. The models developed for the first situation, where density variations are linked to the velocity field, are not necessarily applicable to the second case corresponding to the mixing between fluids (gas or liquid) with different densities. There, the density variations can be related to temperature variations or to mixing of flows with species of different density, for example, gases having different molecular weights. Such flows can also display compressible effects when the velocity is sufficiently high. They again indicated that when the flows are turbulent, the density fluctuates and must be considered as an additional random variable. The averaging technique can either be the Reynolds or the Favre averaging method. In the first case, special correlations involving the density fluctuations also appear in the averaged equations, whereas in the second case these terms are generally hidden and the equations look, at least formally, like the conventional equations obtained for constant density flows. Thus, the effects of density variation must be introduced through a careful examination of existing models. While both methods look very different, not only in the form of the equations but also in the variables chosen to represent the solution, they are both generally suitable and can be applied with equivalent success. In liquid–gas flows, turbulence models for variable density flows must deal with two particular aspects: first, the density ratio can be of the order of 1000 and second, at small scales, there is no dissipation of the density gradient by molecular diffusion. These peculiarities are likely to enhance the effect of density variations and therefore highlight the limitations of conventional models of turbulence. In spray and atomization, liquid properties and ambient gas properties can significantly alter the mean droplet size and distribution. The liquid surface tension and viscosity tend to prevent breakup and instabilities, whereas the gas density will promote instability and breakup due to aerodynamic interaction. Liquid density, while having a smaller overall effect on the flow can

ISSN 2348 – 7968

also alter performance as the higher inertia of the liquid phase [9, 10].In addition to fluid properties, different instability mechanisms are paramount to the atomization process. These instability mechanisms include the Kelvin-Helmholtz instability arising from the interfacial shear across the liquid-gaseous boundary and the Rayleigh-Taylor instability that forms due to the different densities of the two fluids. The Kelvin-Helmholtz instability mechanisms are prevalent mostly in the primary atomization process while the Rayleigh-Taylor instability model is suitable for predicting the secondary breakup regime. Though these models in some aspects provide reasonable predictions of the liquid atomization, they do not account for the liquid turbulence motion observed in certain sprays. Recent experimental investigations and physical modelling studies[11, 12] have indicated that turbulence behaviours within a liquid jet have considerable effects on the atomization process. Such turbulent flow phenomena are encountered in most practical applications of common liquid spray devices.

2. Eulerian model

An entirely Eulerian approach proposed by Vallet et al.[5] treats a two- phase medium as a single continuum where the dense phase is described similarly to a species in a multi-component reactive mixture.

The mass and momentum conservation equations (the 'Navier-Stokes' equations) for general incompressible fluid flows are shown in equations 1 and 2 respectively [13]
Mass conservation

$$\frac{d}{dt}\int_V \rho dV + \int_S \rho v(v - v_b).nds = 0 \qquad 1$$

Momentum conservation

$$\frac{d}{dt}\int_V \rho dV + \int_S \rho v(v - v_b).nds = \int_S (T - pI).nds + \int_V \rho b dV \qquad 2$$

Let $\tilde{Y}_{liq}$ be the liquid mass fraction per unit mass of the two-phase medium, then
Conservation equation for liquid mass fraction [14]

$$\frac{\partial \bar{\rho}\,\tilde{Y}_{liq}}{\partial t} + \frac{\partial \bar{\rho}\,\tilde{u}_j \tilde{Y}_{liq}}{\partial x_j} = \frac{\partial}{\partial x_j}\bar{\rho}\frac{D_t}{Sc_{liq}}\frac{\partial \tilde{Y}_{liq}}{\partial x_j} - \dot{m}_{vap}\tilde{\rho}\tilde{\Sigma} \qquad 3$$

where $\bar{\rho}$ is the Reynold-average density, $\tilde{u}_j$ is the Favre-averaged velocity of both phases,

The mean density $\bar{\rho}$ is related to the Favre averaged liquid mass fraction $\tilde{Y}$ by

$$\frac{1}{\bar{\rho}} = \frac{\tilde{Y}_{liq}}{\rho_l} + \frac{1-\tilde{Y}_{liq}}{\rho_g} \qquad 4$$

where ρ_l and ρ_g are the constant liquid and gas densities respectively. It is assumed that the pressure acting upon both phases is equal.
$\dot{m}_{vap}$ is the mean rate of vaporization per unit surface of the liquid $\tilde{\Sigma}$ is the mean surface area of the gas-liquid interface per unit of two-surface media. Dispersion of the liquid by the turbulence is expressed in the equation by using the turbulent diffusivity D_t and the turbulent Schmidt number as constant $Sc_{liq} = 0.7$

Let $\tilde{\Sigma}$ be the average surface area of the liquid-gas interface per unit mass of two phase medium. The transport equation for the $\tilde{\Sigma}$ can be written as [14]

$$\frac{\partial \bar{\rho}\,\tilde{\Sigma}}{\partial t} + \frac{\partial \bar{\rho}\,\tilde{u}_j\tilde{\Sigma}}{\partial x_j} = \frac{\partial}{\partial x_j}\bar{\rho}\frac{D_t}{Sc_\Sigma}\frac{\partial \tilde{\Sigma}}{\partial x_j} + \frac{\bar{\rho}\tilde{\Sigma}}{\tau_c}\left[1 - \frac{\tilde{\Sigma}}{\Sigma_{eq}}\right] \qquad 5$$

where D_t is the turbulent diffusivity, Sc_Σ is turbulent Schmidt number and is a constant $Sc_\Sigma = Sc_t = 0.7$, τ_c is the rate of surface production and is proportional to turbulence time scale given by

$$\tau_c = C_1\frac{\tilde{k}}{\tilde{\varepsilon}} \qquad 6$$

Σ_{eq} is equilibrium interface area and is related to equilibrium drop size r_{eq} [5, 14] by:

$$\Sigma_{eq} = \frac{3\tilde{Y}_{liq}}{\rho_l r_{eq}}, \qquad r_{eq} = C_r\left(\frac{\bar{\rho}\tilde{Y}_{liq}}{\rho_{liq}}\right)^{2/15}\frac{\eta^{2/5}}{\tilde{\varepsilon}^{2/5}{\rho_{lig}}^{3/5}} \qquad 7$$

where C_r is a constant η is the surface tension of the liquid.
The atomization model eqs.(3) and (5) require a turbulent diffusivity and an integral scale τ_c and the standard k-ε turbulence model was used to calculate these variables as well as providing closure of the fluid dynamics transport equations[15].
Once $\tilde{\Sigma}$ is calculated, the Sauter mean diameter (SMD) d_{32} and the number density n can be found as:

$$d_{32} = \frac{6\tilde{Y}_{liq}}{\rho_{liq}\tilde{\Sigma}} \qquad n = \frac{{\rho_{liq}}^2\,\tilde{\Sigma}^3}{36\pi{\tilde{Y}_{liq}}^2} \qquad 8$$

3. Numerical procedure

Computations are performed courtesy CFD code STAR CCM+10.02.010-R8 for Windows 64 using User-Defined Functions (UDF) to introduce the transport equation for the liquid mass fraction and the average density. The equations are solved using the finite-volume method in association with the SIMPLE algorithm and the Second Order Upwind scheme. The SIMPLE algorithm uses a relationship between velocity and pressure corrections to enforce mass conservation and to obtain velocity and pressure field. The Second Order discretization is more accurate than the First Order upwind scheme and more suited for

ISSN 2348 – 7968

practical engineering problems. Two equations standard k-ε model has been adopted for the computation of turbulent behaviour in the liquid since there is no conclusive information available in the literature concerning accurate and suitable modification of the k-ε model for a two phase confined swirling flow. The geometry shown in Fig 1 is created using the 3D-CAD model in STAR-CCM+ and surfaces are split by patch of colours. The model consists of two parts the nozzle part which is attached to the computation domain just to study the flow at the exist orifice of 2mm in diameter. The computation domain dimensions are large so that the outlet boundary conditions do not affect the flow.

Three-dimensional calculations are carried out on the flow through the velocity inlet2 of 2mm diameter with liquid ($\rho_l = 800kg/m^3$) and air ($\rho_g = 1.30kg/m^3$) through velocity inlet1 having 2mm of diameter as shown in Fig.2. The walls represent the solid walls of the nozzle and the computation domain. The standard wall functions are used to model the near-wall regions with no-slip conditions. Pressure outlet is specified for the flow out. The inlet boundary conditions used to perform the calculations for the liquid are 3 bars for the injection pressure, 1 for liquid mass fraction, 10% for turbulence intensity, 0.04mm for turbulent length scale and 10.0 m/s for the velocity magnitude. And for the two air inlets the values remain the same except for the velocity magnitude which is 100 m/s. The outlet boundary conditions are 1% for turbulent intensity, mass fraction of one for both liquid and air and 0.01m for the turbulent length scale. A nom-uniform mesh grid composed of 757429 polyhedral cells and 5152033 faces is used for the computation and shown in Fig.3. The distribution of the mesh is done such that the swirl chamber and the cylinder have fine and coarse meshes respectively. The refined grid spacing on the swirl chamber was about 0.15 mm and coarse mesh of 1.0 mm on the computation domain with a growth factor of 2.0.This is to reduce the computational time and for 3.20GHz intel(R) Xeon(R) processor to accommodate. The total computational time was about three (3) days.

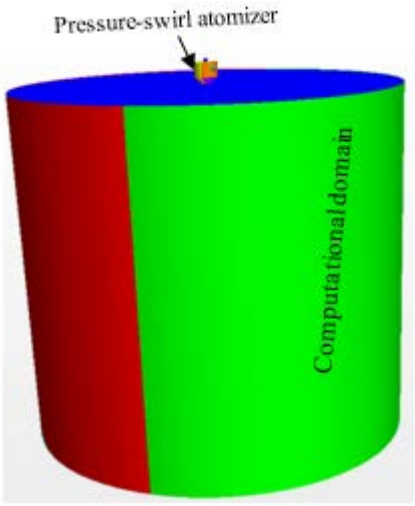

Fig.1 Geometry in three dimension

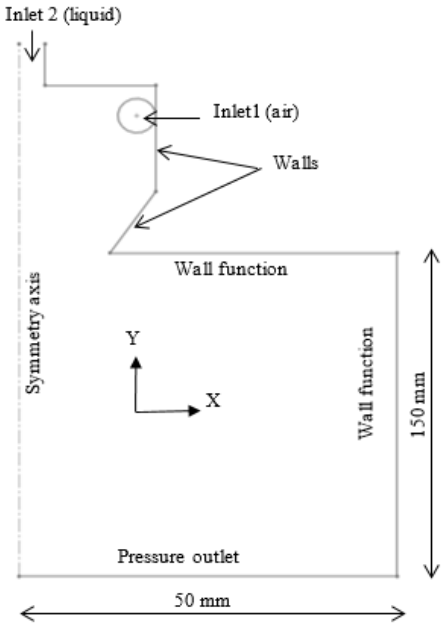

Fig.2.The computational domain and boundary conditions

ISSN 2348 – 7968

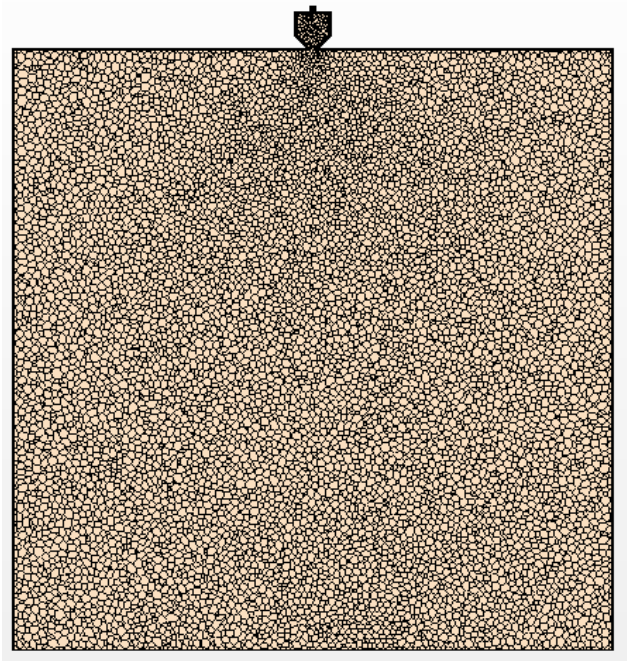

Fig.3. Mesh on vertical plane through the atomizer and domain

4. Results and discussion

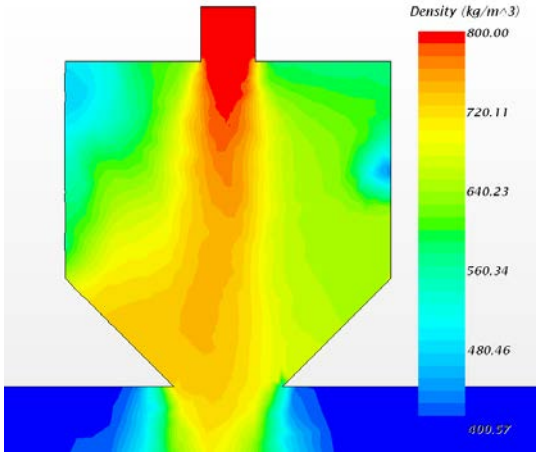

Fig. 4. Scalar scene for density

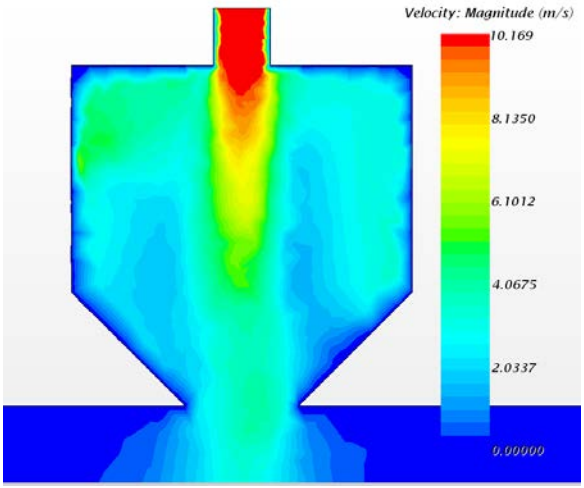

Fig. 5. Scalar scene for velocity magnitude

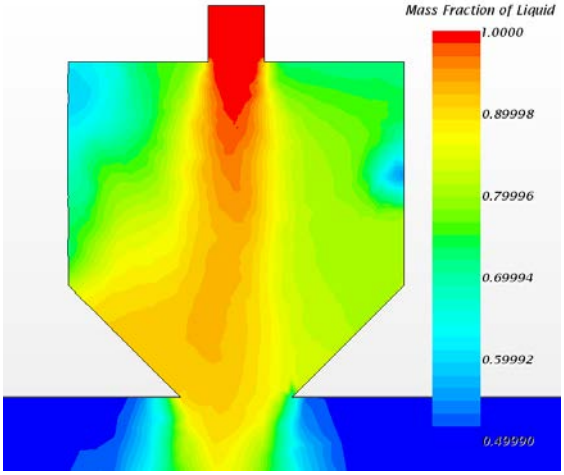

Fig.6. Scalar scene for mass fraction of liquid

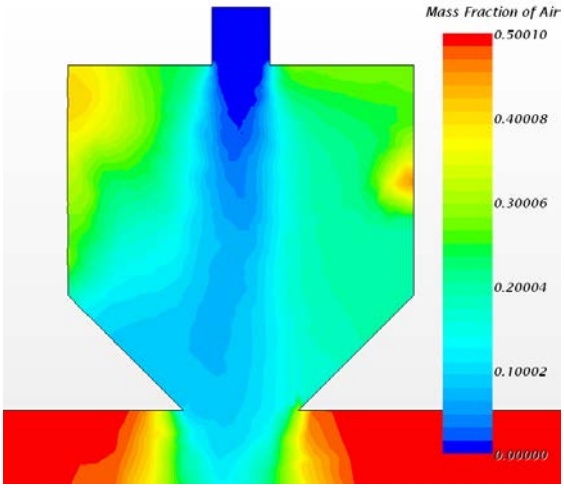

Fig. 7. Scalar scene for mass fraction of air

ISSN 2348 – 7968

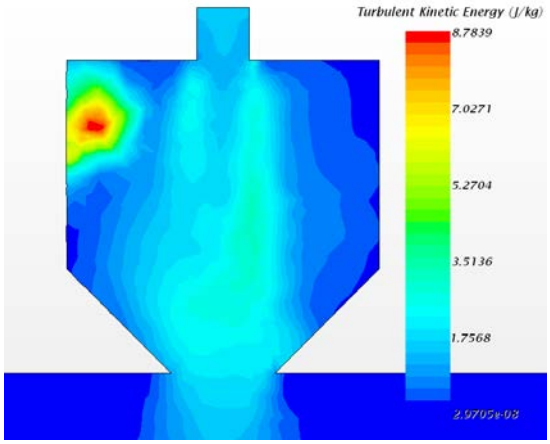

Fig. 8. Scalar scene for turbulent kinetic energy

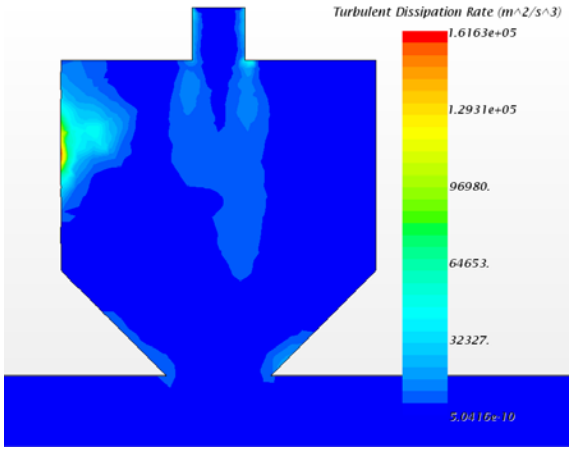

Fig. 9. Scalar scene for turbulent dissipation rate

Fig.4-9 shows the various scalar scenes on the vertical plane when the transport equation for the liquid mass fraction and average density were defined. Fig 4 shows the contour plot of density. The blue colour corresponds to the lowest density and the red colour representing the maximum value for the density distribution can be observed in the vicinity of the liquid entry into the atomizer. The density variation can be seen in between these two limits and is quite large in relation to the maximum and minimum values of the density distributions. Fig.6 presents the liquid mass fraction field $\tilde{Y}$.The liquid mass fraction lies between 0 and 1. Value 1 (in red) represents the liquid and value 0 represents air (in blue) as shown in Fig. 7 for the air mass fraction distributions. The value of the mass fraction of the liquid decreases inside the atomizer as the liquid penetrates the air. Outside the spray there is only air. The flow field for the velocity magnitude is shown in Fig 5 and indicate that regions of relatively high velocities in the liquid are found to be in the atomizer compared to the computational domain. Conical spray is clearly visible, minimum values are found downstream the spray. Figs 8 and 9 shows the contour plots of turbulent kinetic energy and turbulent dissipation rate. It can be observed that these turbulence fields show some significant differences in relation to density variations.

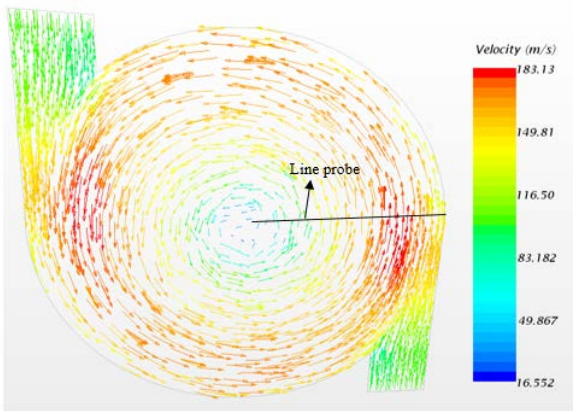

Fig. 10. Velocity profile in the swirl chamber

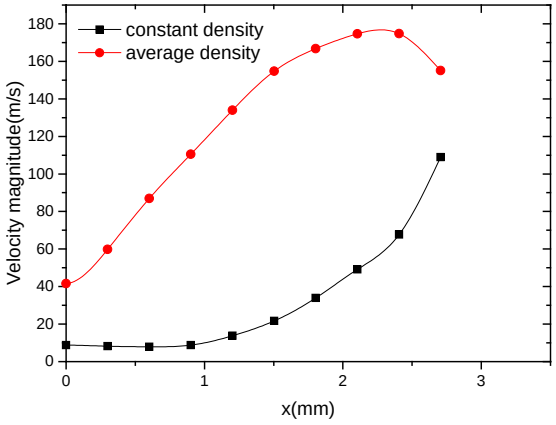

Fig.11 Density variations on velocity magnitude

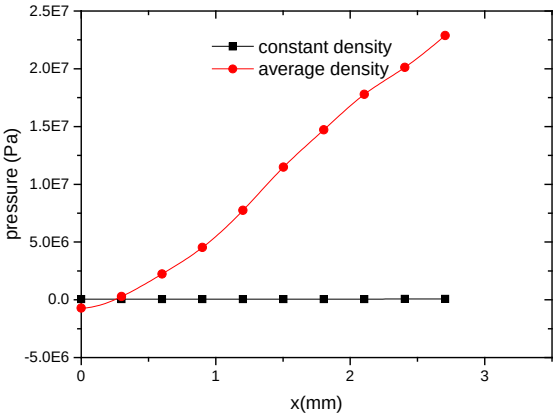

Fig.12 Density variations on pressure profile on the internal walls of the atomizer

The Fig 10 shows the distributions of velocity magnitudes in the swirl chamber for the average density definition for the liquid and air using user defined functions. The profiles show clearly the swirl motion is achieved in the atomizer and the velocity is higher near the walls as indicated by the red colour in the distribution and lower around the core of the chamber. Fig.11 shows the graphs of velocity magnitude positions on the probe line for linearized

ISSN 2348 – 7968

equation of state (constant density) in the STAR-CCM+ and average density defined for the liquid and air using user defined functions. The general profile of the velocity magnitudes taken on the probe line for the model are quite similar to the measured velocity profiles at the inlet level by Horvay and Leuckel [16]. It can be observed that the velocity magnitudes for the average density is high at all positions than its counterpart for the equation of state (constant density) which indicates that density variations affect the velocity distributions in the swirl chamber of the atomizer. The pressure distributions of the liquid on the internal walls of the atomizer for the two densities have been compared as shown in Fig. 12. It can be deduced from the graph that the pressure increases for the average density when compared to the pressure for the constant density which is almost constant on the probe line.

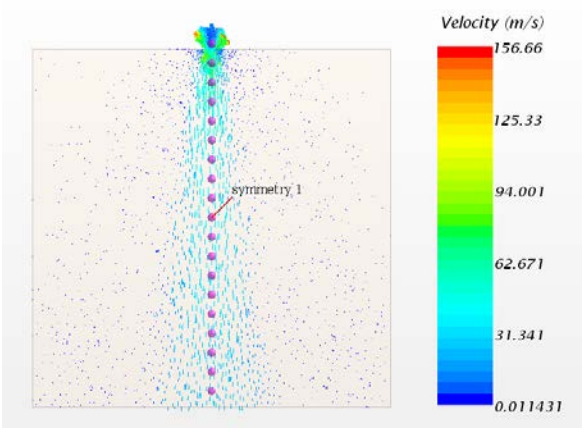

Fig.13 Velocity profiles on a vertical plane through the atomizer

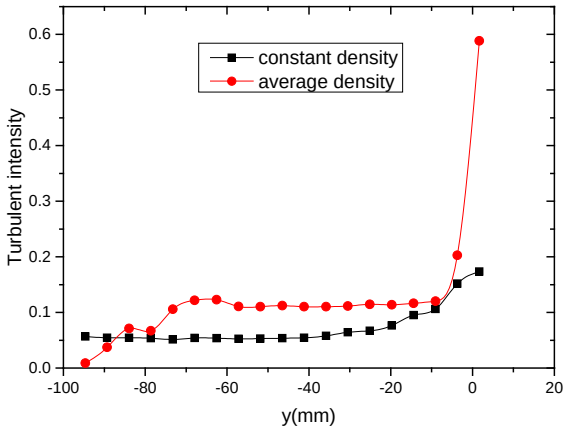

Fig. 14 The effect of density variations on turbulent intensity

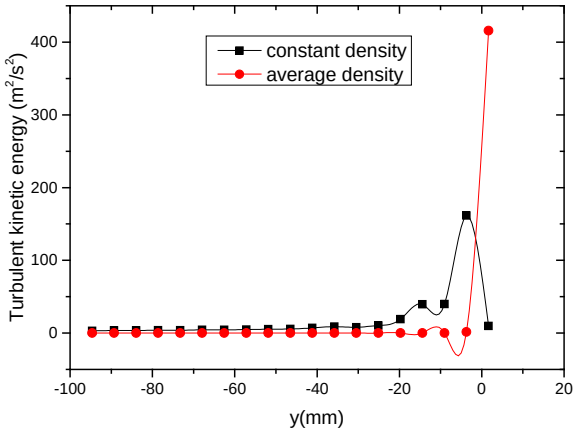

Fig.15 The effect of density variations on turbulent kinetic energy

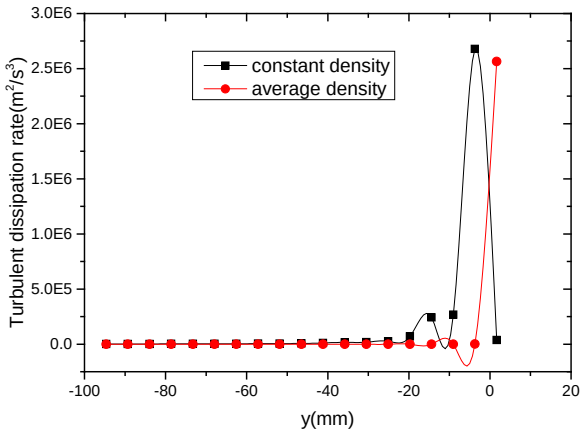

Fig. 16 The effect of density variations on turbulent dissipation rate

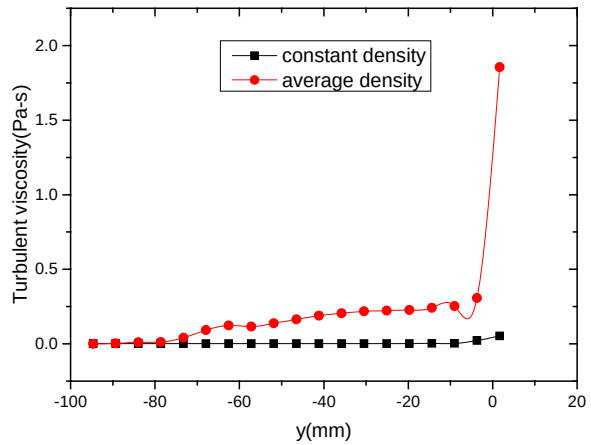

Fig. 17 The effect of density variations on turbulent viscosity

ISSN 2348 – 7968

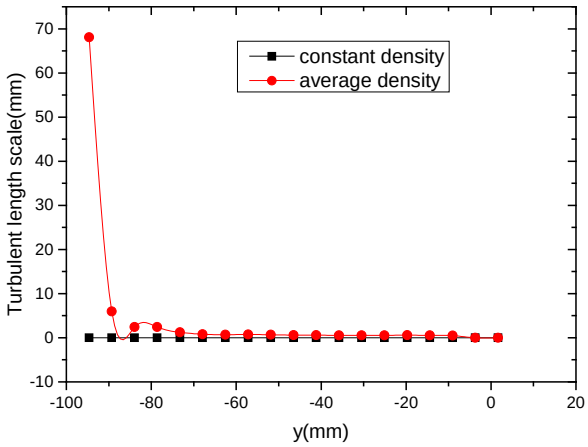

Fig. 18 The effect of density variations on turbulent length scale

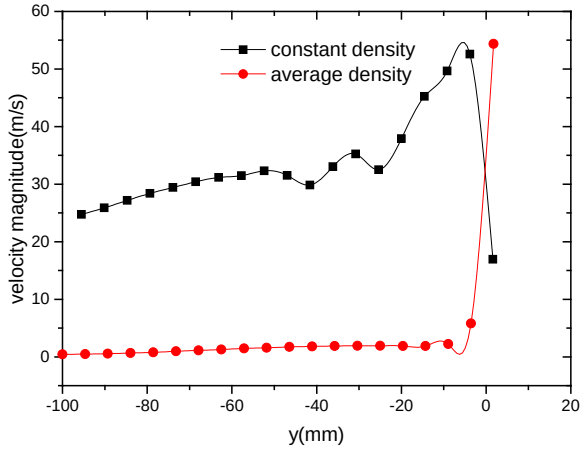

Fig. 19 The effect of density variations on velocity magnitude

The Fig 14-19 show the graphs of turbulence and flow fields on the symmetry line of the vertical plane for the constant and average densities for the model. The x- axis represents the positions on the symmetry axis and the vertical axis shows the turbulent and the flow fields. The velocity magnitude shown in Fig 13 indicates that the correct flow directions have been achieved and turbulent parameters are evaluated on the symmetry line shown on it. The turbulent intensity shown in Fig 14 is higher in the spray centre axis for the average density than the constant density for the same axial locations. Low values of intensity are observed in the computational domain. High turbulent kinetic energies can be seen in the atomizer for the two densities and this may be due to high turbulent intensity of 10% specified at inlet2. In the computational domain, low values of energy are found for the two densities. The maximum value for the rate of dissipation of turbulent kinetic energy for the average density is 2.5E6 m^2/s^2 and negative value is observed just below the atomizer exit as shown in Fig 16. Maximum and minimum values for the turbulent viscosity are 1.8 Pa.s and zero for the average density and it remains almost zero for the constant density. Significant changes are observed in the integral length scale at the downstream on the symmetry line for the two densities (Fig 18). The flow velocity is high in the atomizer for the two densities and decreases quite linearly in the computational domain with the constant density flow exhibiting high values than the average density flow as shown in Fig 19. It can be concluded that some turbulent quantities show noticeable changes for the two densities and some slight differences which clearly indicates that variable densities affect turbulence behaviour in a flow field.

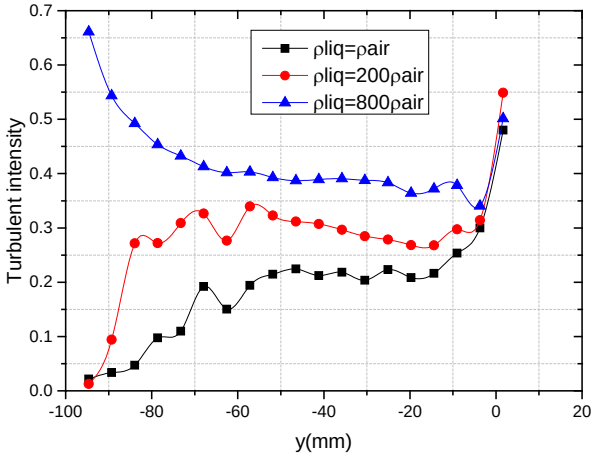

Fig. 20 The effect of variation of liquid density on the turbulent intensity

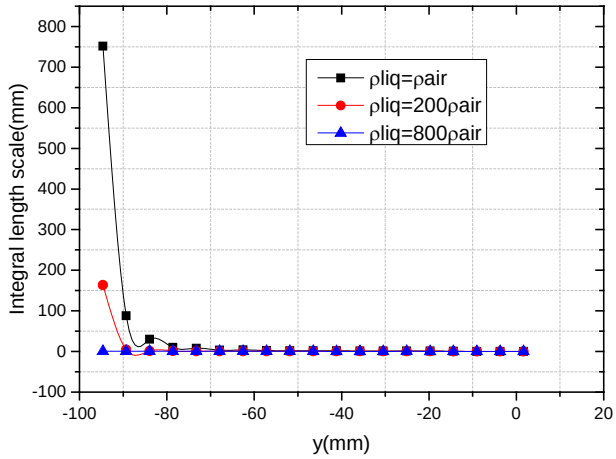

Fig. 21 The effect of variation of liquid density on integral length scale

ISSN 2348 – 7968

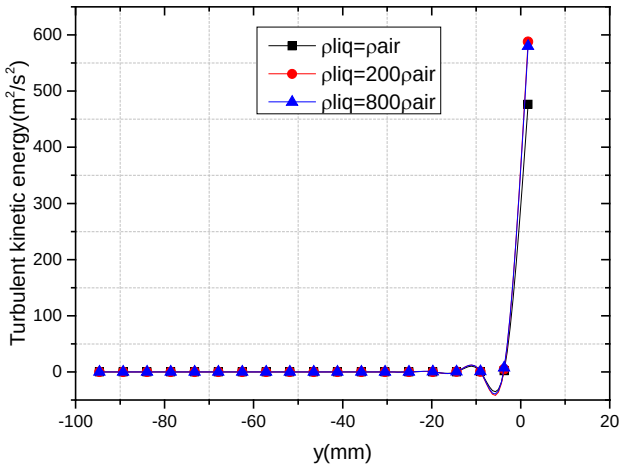

Fig. 22 The effect of variation of liquid density on turbulent kinetic energy

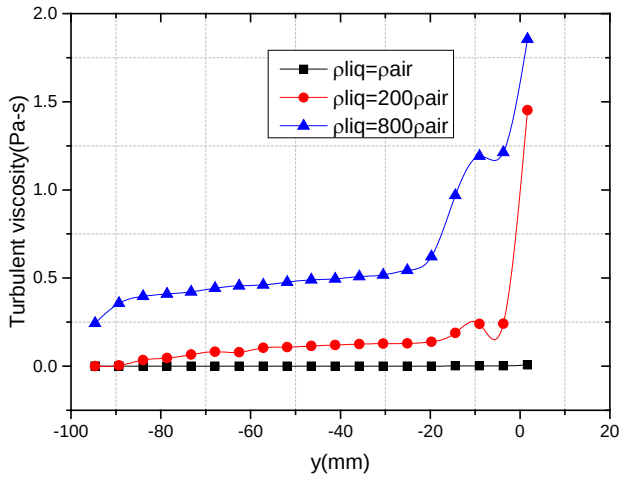

Fig. 23 The effect of variation of liquid density on turbulent viscosity

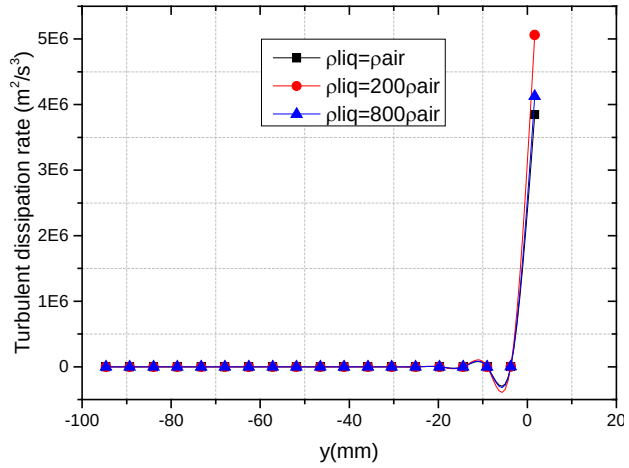

Fig. 24 The effect of variation of liquid density on turbulent dissipation rate

The graphs in Figs 20- 24 show the influence of changes in the liquid density on the turbulent quantities for the simulation. Three liquid density values (1) when $\rho_{liq} = \rho_{air}$ (2) when $\rho_{liq} = 200\rho_{air}$ and (3) when $\rho_{liq} = 800\rho_{air}$ were compared with all other flow variables remaining constant. Fig 20 presents the effect of density variations on turbulent intensity on a section plane for the liquid and air modelled as a single multicomponent species when all the equations were defined. It can be observed that the turbulent intensity increases with increasing density ratios but the turbulent length scale rather increases with decreasing density ratios. Large density variations on the length scale can be seen downstream of the spray on the symmetry line. The turbulent kinetic energy also shows increases when the liquid density varies from 1.30 kg/m^3 to 1040 kg/m^3. These high values of turbulent kinetic energies can be seen in the atomizer and low turbulent kinetic energies are noticeable few millimetres from the atomizer exit. The increase in density ratios also give rise to significantly increase in the turbulent viscosity as shown in Fig 23. High rates of dissipation of the turbulent kinetic energy are higher in the atomizer than the computation domain in relation to variations in density ratios. It can be deduced clearly from the results that the increase in liquid density reveals changes in individual turbulent parameters and the changes are disproportionate.

5. Conclusion

In the paper, entirely Eulerian one fluid model has been implemented in STAR-CCM+ to analyse the effect of density ratios on the turbulence fields. Average density for the two fluids have been defined and a transport equation tracking the transport of liquid mass fraction $\tilde{Y}_{liq}$ is used to model the turbulent mixing of liquid. With these quantities, flow and turbulent fields are generated, liquid and air density ratios varied and the turbulent parameters are evaluated on the symmetry axis.

Reference

[1] Elghobashi, S. and T. Abou-Arab, *A two-equation turbulence model for two-phase flows.* Physics of Fluids (1958-1988), 1983. **26**(4): p. 931-938.

[2] Yeung, W.-S., *Similarity analysis of gas-liquid spray systems.* Journal of Applied Mechanics, 1982. **49**(4): p. 687-690.

[3] Abbas, A., S. Koussa, and F. Lockwood. *The prediction of the particle laden gas flows.* in *Symposium (International) on Combustion.* 1981. Elsevier.

[4] Crowe, C.T., M.P. Sharma, and D.E. Stock, *The particle-source-in cell (PSI-CELL) model for gas-droplet flows.* Journal of Fluids Engineering, 1977. **99**(2): p. 325-332.

ISSN 2348 – 7968

[5] Vallet, A., Burluka, AA and R. Borghi, *Development of a Eulerian model for the "atomization" of a liquid jet.* Atomization and sprays, 2001. **11**(6).

[6] Ruffin, E., *Etude de jets turbulents à densité variable à l'aide de modèles de transport au second ordre*. 1994.

[7] Brown, G.L. and A. Roshko, *On density effects and large structure in turbulent mixing layers.* Journal of Fluid Mechanics, 1974. **64**(04): p. 775-816.

[8] Demoulin, F.-X., et al., *A new model for turbulent flows with large density fluctuations: application to liquid atomization.* Atomization and Sprays, 2007. **17**(4).

[9] Lefebvre, A., *Atomization and sprays*. Vol. 1040. 1989: CRC press.

[10] Lefebvre, A.H. and D. Hallal, *Gas Turbine Alternative Fuels and Emissions.* CRC, Boca Raton, FL, 2010.

[11] Trinh, H.P., C. Chen, and M. Balasubramanyam, *Numerical simulation of liquid jet atomization including turbulence effects.* Journal of engineering for gas turbines and power, 2007. **129**(4): p. 920-928.

[12] Belhadef, A., et al., *Pressure-swirl atomization: Modeling and experimental approaches.* International Journal of Multiphase Flow, 2012. **39**: p. 13-20.

[13] Guide, U., *Star-CCM+ Version 8.04.* CD-adapco-2013, 2013.

[14] Beheshti, N., A.A. Burluka, and M. Fairweather, *Assessment of Σ− Y liq model predictions for air-assisted atomisation.* Theoretical and Computational Fluid Dynamics, 2007. **21**(5): p. 381-397.

[15] Beheshti, N., A. Burluka, and M. Fairweather. *Atomisation In Turbulent Flows: Modelling For Application*. In *Tsfp Digital Library Online*. 2003. Begel House Inc.

[16] Horvay, M. and W. Leuckel, *Experimental and theoretical investigation of swirl nozzles for pressure-jet atomization.* German chemical engineering, 1986. **9**(5): p. 276-28

Author's Profile

Sherry K. Amedorme: I am currently a PhD student in Mechanical Engineering at the University of Leeds, UK. l research into the application of CFD in internal combustion engines, l am also a lecturer in the Department of Electrical and Automotive Technology Education at College of Technology Education of the University of Education, Winneba (UEW). I hold BSc and MSc degrees in Mechanical Engineering from the Kwame Nkrumah University of Science and Technology, Kumasi, Ghana (KNUST). I have City and Guilds of London Certificate in motor vehicle and a Certificate in Technology Education from the College of Technology Education, Kumasi of the University of Education, Winneba.

Joseph Apodi: I am a lecturer in the Department of Agricultural Engineering of Bolgatanga Polytechnic, in the Upper East Region of Ghana. I hold Masters of Technology Education (M.TECH.) in Mechanical Technology from the University of Education Winneba (UEW) and a BSc in Mechanical Engineering from the Kwame Nkrumah University of Science and Technology, Kumasi, Ghana (KNUST). I also have Mechanical Engineering Technician Part I, II, and III Certificates from Kumasi and Accra Polytechnic respectively as well as Full Technological Certificate (FTC) from the Technical Examination Unit, Accra Ghana.